Received: 3 September 2023 | Revised: 6 March 2024 | Accepted: 12 March 2024

DOI: 10.1111/cas.16164

Cancer Science WILEY

ORIGINAL ARTICLE

Adrenergic microenvironment driven by cancer-associated Schwann cells contributes to chemoresistance in patients with lung cancer

Yusuke Otani[1,2,3] | Haruyoshi Katayama[4] | Yidan Zhu[1] | Rongsheng Huang[5] | Takafumi Shigehira[6] | Kazuhiko Shien[1] | Ken Suzawa[1] | Hiromasa Yamamoto[1] | Tadahiko Shien[1] | Shinichi Toyooka[1] | Atsushi Fujimura[6,7]

[1]Department of General Thoracic Surgery and Breast and Endocrinological Surgery, Okayama University Graduate School of Medicine, Dentistry and Pharmaceutical Sciences, Kita-ku, Okayama, Japan

[2]Department of Pathology, Beth Israel Deaconess Medical Center, Boston, Massachusetts, USA

[3]Harvard Medical School, Boston, Massachusetts, USA

[4]Department of Orthopaedic Surgery, Okayama University Graduate School of Medicine, Dentistry and Pharmaceutical Sciences, Kita-ku, Okayama, Japan

[5]Department of Trauma Orthopedics, The Second Hospital of Dalian Medical University, Dalian, Liaoning, China

[6]Department of Cellular Physiology, Okayama University Graduate School of Medicine, Dentistry and Pharmaceutical Sciences, Kita-ku, Okayama, Japan

[7]Neutron Therapy Research Center, Okayama University, Kita-ku, Okayama, Japan

Correspondence
Atsushi Fujimura, Department of Cellular Physiology, Okayama University Graduate School of Medicine, Dentistry and Pharmaceutical Sciences, 2-5-1 Shikata-cho, Kita-ku, Okayama, 700-8558, Japan.
Email: atsushi.fujimura@okayama-u.ac.jp

Funding information
Japan Agency for Medical Research and Development, Grant/Award Number: JP19cm0106143 and JP22cm0106179; Naito Foundation; Japan Society for the Promotion of Science, Grant/Award Number: JP22H03162, JP22K09004 and JP23K06676

Abstract

Doublecortin (DCX)-positive neural progenitor-like cells are purported components of the cancer microenvironment. The number of DCX-positive cells in tissues reportedly correlates with cancer progression; however, little is known about the mechanism by which these cells affect cancer progression. Here we demonstrated that DCX-positive cells, which are found in all major histological subtypes of lung cancer, are cancer-associated Schwann cells (CAS) and contribute to the chemoresistance of lung cancer cells by establishing an adrenergic microenvironment. Mechanistically, the activation of the Hippo transducer YAP/TAZ was involved in the acquisition of new traits of CAS and DCX positivity. We further revealed that CAS express catecholamine-synthesizing enzymes and synthesize adrenaline, which potentiates the chemoresistance of lung cancer cells through the activation of YAP/TAZ. Our findings shed light on CAS, which drive the formation of an adrenergic microenvironment by the reciprocal regulation of YAP/TAZ in lung cancer tissues.

KEYWORDS
adrenaline, cancer-associated Schwann cells, doublecortin, microenvironment, YAP/TAZ

Abbreviations: CAS, cancer-associated Schwann cells; CSC, cancer stem cell; DbH, dopamine beta-hydroxylase; DCX, doublecortin; DDC, DOPA decarboxylase; INA, alpha-internexin; Nf-h, neurofilament heavy polypeptide; NGFR, p75 nerve growth factor receptor; PNMT, phenylethanolamine *N*-methyltransferase; PSA-NCAM, polysialic acid-neural cell adhesion molecule; TAZ, transcriptional co-activator with PDZ-binding motif; TH, tyrosine hydroxylase; YAP, yes-associated protein; yNSC, YAP-induced neural stem-like cells.

1 | INTRODUCTION

Recent advances in multidisciplinary treatment methods, including molecular-targeted drugs, have successfully improved the prognosis of lung cancer.[1–3] However, the prognosis of patients with metastasis or recurrence remains poor.[4] Cancer stem cell populations are the main cause of metastasis and recurrence.[5,6] They are characterized by a high self-renewal, maintenance of an undifferentiated state, tumorigenesis, and chemo-/radioresistance and are thus considered a promising therapeutic target.[7–10]

Among the determinants of cancer stemness, the tumor microenvironment has been widely investigated for its association with the maintenance of CSCs.[11–13] The cancer microenvironment comprises cellular components, such as tumor-associated fibroblasts and tumor-associated macrophages,[14,15] gaseous components such as hypoxia,[16,17] and liquid components, such as cytokines and metabolites.[18,19] The importance of catecholamines among the liquid components of the cancer microenvironment has been recently reported.[20–22] In patients with breast cancer, a stress-induced increase in blood adrenaline enhances cancer stemness via the elevation of CSC-related factors, including c-*myc* and beta-catenin.[20] We also previously reported that, in malignant peripheral nerve sheath tumor (MPNST), adrenaline treatment enhances tumor stemness by inducing activation of YAP/TAZ,[23] which is the Hippo pathway transducer and also known as a CSC-related factor.[24–26]

When considering the pathways by which adrenaline acts on tumor tissue, adrenaline in the blood is the most likely route; however, other possibilities may exist. For instance, it has recently been reported that DCX-positive neural progenitor cells in the central nervous system can flow directly into tumor tissue and become engrafted and differentiated into sympathetic neuron-like cells in patients with prostate cancer.[27] Because these cells reportedly express TH, a rate-determining factor of catecholamine synthesis, they may be able to synthesize and secrete adrenaline directly into tumor cells and thus possibly contribute to cancer progression.

In a preliminary experiment we investigated the possibility of TH-positive sympathetic nerve fibers infiltrating lung cancer tissue. However, unlike previous reports, we did not observe clear evidence of TH-positive nerve fiber infiltration in human lung cancer tissues. Instead, we identified TH-positive cell bodies in lung cancer tissues. As DCX-positive cells differentiate into sympathetic neuron-like cells within tumor tissues, as mentioned above,[27] we decided to investigate the role of DCX-positive cells in lung cancer tissues. Interestingly, unlike prostate cancer, DCX-positive cells in lung cancer tissue may be CAS in the peripheral tissues and we investigated the molecular mechanism of the process of acquisition of their traits. These findings indicate the importance of Schwann cells as cellular components of the tumor microenvironment and contribute to the advancement of therapeutic strategies targeting the cancer microenvironment.

2 | MATERIALS AND METHODS

2.1 | Lineage-tracing experiment

For lineage-tracing experiments, we prepared a *P0-cre/loxP-stop-loxP-tdTomato* mouse line by crossing a mouse line that expressed under the P0 promoter and a mouse line that expresses tdTomato only under Cre expression with loxP-stop-loxP-tdTomato. The mice were transvenously inoculated with 1×10^5 cells/100 μL of the 3LL cell line. Three weeks later, xenograft tumors were excised and subjected to immunofluorescence analysis. Animal experiments were performed with permission from and in accordance with all guidelines published by the committees of Okayama University (approval number: OKU-2021726 for animal usage and 20,028 for recombinant DNA experiments on transgenic mice).

2.2 | Statistical analyses

An unpaired two-tailed *t*-test was used to assess the differences between both groups. A one-way analysis of variance with Tukey's multiple comparisons post hoc test was used to compare more than two groups. The log-rank test was used for survival analysis. A *p*-value <0.05 was considered statistically significant. All analyses were performed using the JMP Pro 16 software (SAS Institute Japan, Tokyo, Japan).

For the other materials and methods, see Supporting Information and Tables S1 and S2.

3 | RESULTS

3.1 | DCX-positive cells are found in primary human lung cancer tissues

The presence of DCX-positive cells in lung cancer tissues was examined by immunostaining. DCX-positive cells were present in all

FIGURE 1 DCX-positive cells are found in primary human lung cancer tissues. (A–D) Representative images of immunofluorescence analyses using anti-DCX and anti-pan-cytokeratin antibodies on human lung cancers. DCX-positive cells are present in an adenocarcinoma (A), squamous-cell carcinoma (B), small-cell carcinoma (C), and large-cell neuroendocrine carcinoma (D). Scale bars: 50 μm in (A) and 20 μm in (B–D). $n=26$ (A), $n=26$ (B), $n=9$ (C), $n=3$ (D). (E) In normal human lung tissue, there are no DCX-positive cells. Scale bar: 20 μm. $n=3$. (F) Number of cases with DCX-positive cells per each histological type of human lung cancer. (G) The distribution of the number of DCX-positive cells per field is shown. (H) Boxplot graph describing that the number of DCX-positive cells per field of view is significantly higher in patients with a larger tumor invasive diameter (>2 cm) (red, *right*) than in the smaller cases (<2 cm) (blue, *left*) ($p=0.0038$). (I) Representative image of an immunofluorescence analysis using an anti-DCX antibody (green) and an anti-macrophage marker (S100A9 + Calprotectin) (red). Scale bar: 20 μm. (J, K) DCX-positive cells express undifferentiated neural markers, PSA-NCAM (J) and INA (K). Scale bars: 20 μm. $n=3$, each.

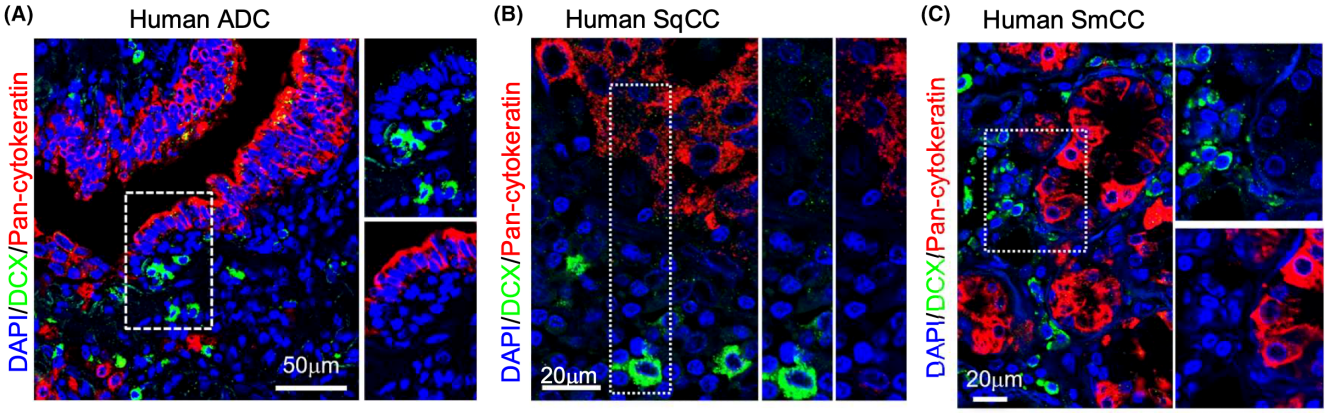

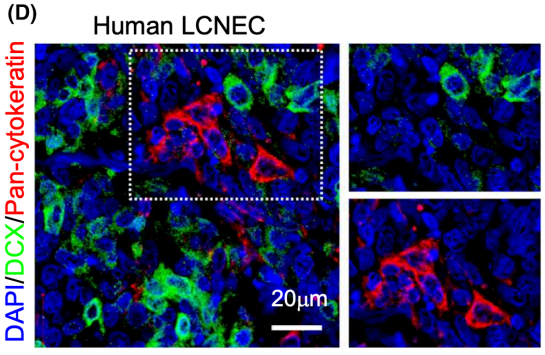

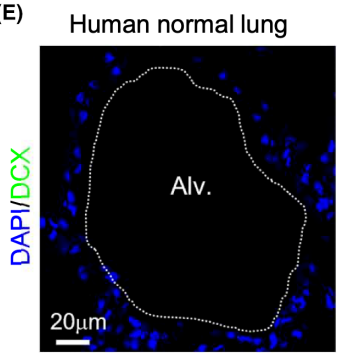

(F)

Histology	Presence of DCX⁺ cells
ADC	23/26
SqCC	21/26
SmCC	8/9
LCNEC	3/3

(cases)

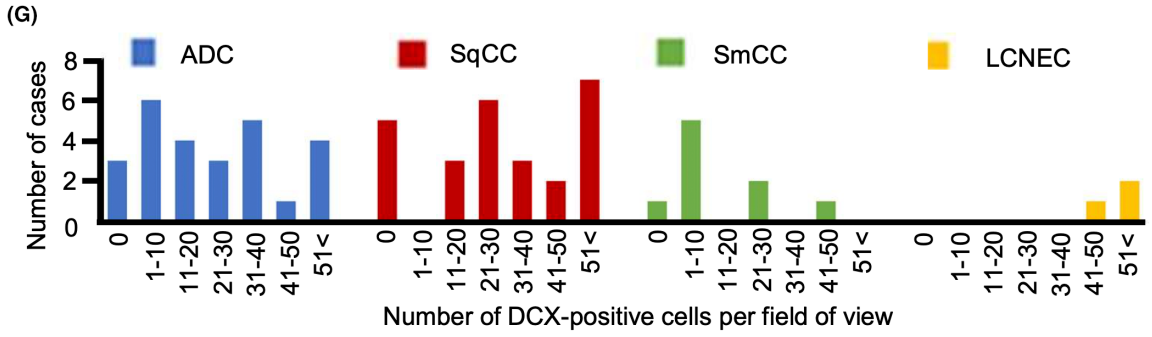

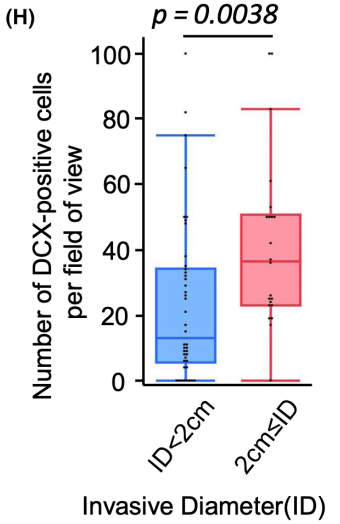

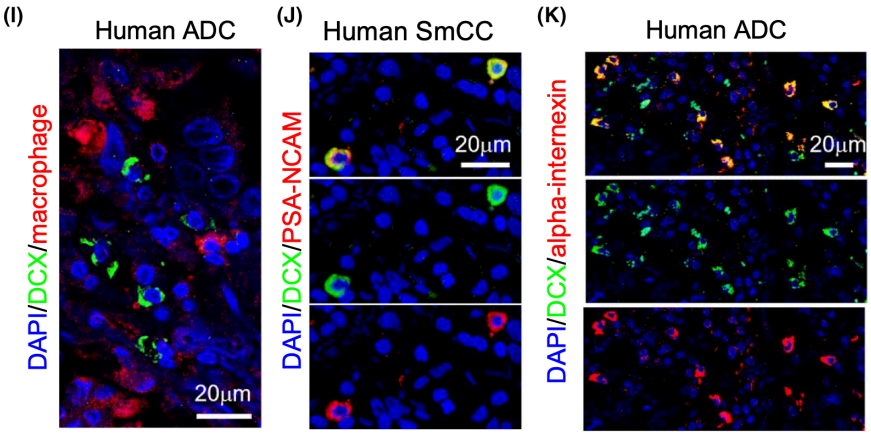

histological types of adenocarcinoma, squamous-cell carcinoma, small-cell carcinoma, and large-cell neuroendocrine carcinoma (Figure 1A–D), but not in normal lung tissue (Figure 1E). The number of DCX-positive cells per histological type of lung cancer is shown in Figure 1F, and the distribution of DCX-positive cells per field of view in each case is shown in Figure 1G. In lung cancer, the number of DCX-positive cells per field of view was significantly higher in cases with larger tumor diameters (>2 cm) than in those with smaller tumor diameters (<2 cm) (Figure 1H). DCX-positive cells in lung cancer were not stained by pan-cytokeratin (Figure 1 A–D) or by macrophage markers such as anti-S100A9 + Calprotectin (Figure 1I), suggesting that these cells were not cancer cells or macrophages. In a previous report on prostate cancer, DCX-positive cells in cancer tissues expressed markers of neural progenitor-like states such as PSA-NCAM and INA. DCX-positive cells in lung cancer tissues also expressed these markers (Figure 1J,K). These data suggest that DCX-positive cells, derived from cells of the nervous system, are commonly present in the major pathological subtypes of lung cancer.

3.2 | DCX-positive cells in lung cancer tissue express Schwann cell markers

We subsequently sought to determine the origin of DCX-positive cells in lung cancer tissues. Lung tissue is rich in sensory, sympathetic, and parasympathetic nerves.[28] Schwann cells are localized around the axons of these nerve fibers and are known to contribute to the maintenance of their respective neuronal functions or repair of neuronal damage.[29,30] Moreover, Schwann cells reportedly have high plasticity and acquire neural crest-derived stem cell-like cell characteristics.[31,32] Based on these reports, we hypothesized that DCX-positive cells in lung cancer tissue are either dedifferentiated or transdifferentiated from Schwann cells originally present in lung tissue. Schwann cells are localized mainly in the vicinity of bronchioles in normal lung tissue.[33] We performed the immunostaining of normal mouse lung tissue using the Schwann cell marker S100β antibody and confirmed that S100β-positive cells were localized around the bronchiole (Figure 2A). S100β-positive cells were also found along the visceral pleura, suggesting nerve innervation in this area (Figure 2A). These S100β-positive cells did not express DCX (Figure 2A).

Subsequently, we performed immunostaining of human lung cancer specimens using the S100β and DCX antibodies. We confirmed S100β-positive cells in the lung cancer tissues (Figure 2B–E). Interestingly, many DCX-positive cells were located in proximity to S100β-positive cells (Figure 2C–E), and some cells co-expressed DCX and S100β (Figure 2B, arrows). Immunostaining using the p75 NGFR antibody, another Schwann cell marker, confirmed similar results (Figure 2F). These results suggest that Schwann cells in the lung may acquire the DCX positivity in cancer tissues.

3.3 | Lineage-tracing experiments reveal that Schwann cells acquire the DCX positivity in lung cancer

To examine the possibility that the DCX-positive cells in lung cancer tissues are Schwann cells, we conducted lineage-tracing experiments. We generated a *P0-cre/loxP-stop-loxP-tdTomato* mouse line by crossing a mouse line expressing Cre recombinase under the P0 promoter, a known promoter that is active in Schwann cells, and a mouse line expressing tdTomato only under Cre expression with *loxP-stop-loxP-tdTomato* (Figure 3A). Immunofluorescence analysis using anti-DsRed antibodies, which recognize tdTomato protein in paraffin-embedded samples, showed that, in the normal lung tissue of this model, the tdTomato signal was localized in the peribronchial and visceral pleura, and the tdTomato signal was consistent with S100β, supporting the immunostaining results of Figures 2A and 3B. The tdTomato signal was also identified in the vicinity of nerve fibers in the peribronchial area, as shown by immunostaining with an antibody of neuron fiber marker Nf-h, confirming that the tdTomato signals properly indicate Schwann cells (Figure 3C). These tdTomato-positive cells did not express Dcx (Figure 3B), as shown in Figure 2A. Furthermore, the neural progenitor cell population ($Sox2^+/Dcx^+$) in the subventricular zone of the cerebrum of this mouse model did not express tdTomato (Figure S1). To prepare a mouse model of lung cancer xenografts using the *P0-cre/loxP-stop-loxP-tdTomato* mouse line, mice were inoculated transvenously with 1×10^5 cells/100 μL of 3LL, a murine Lewis lung cancer cell line of the same strain (Figure 3D). Immunofluorescence analysis of tumor tissues showed that tdTomato-positive cells exhibited positive staining for Dcx, S100β, and Nf-h (Figure 3E,F, arrowheads). Co-staining with DCX, S100β, and NF-H was observed in a human primary lung adenocarcinoma specimen (Figure 3G). These data indicate that the DCX-positive cells in tumor tissue are Schwann cells and that some of the DCX-positive cells exhibited positive staining for the neuronal marker NF-H.

3.4 | Schwann cells acquire the DCX positivity via YAP/TAZ signaling

We subsequently explored the mechanism by which Schwann cells acquire DCX positivity in lung cancer tissues. In a previous study, the Hippo pathway effector YAP/TAZ was a factor that caused the dedifferentiation of all cell types, including neural cells.[34] Therefore, we hypothesized that the acquisition of new traits of Schwann cells in lung cancer tissues is promoted by YAP/TAZ signaling. To verify this, we performed an immunofluorescence analysis of normal lung tissue of *P0-cre/loxP-stop-loxP-tdTomato* mice and a lung cancer xenograft model with the transvenous injection of 3LL, as shown in Figure 3. As expected, no Yap expression was observed in Schwann cells in the normal lungs of *P0-cre/loxP-stop-loxP-tdTomato* mice (Figure 4A), whereas abundant Yap expression was observed in

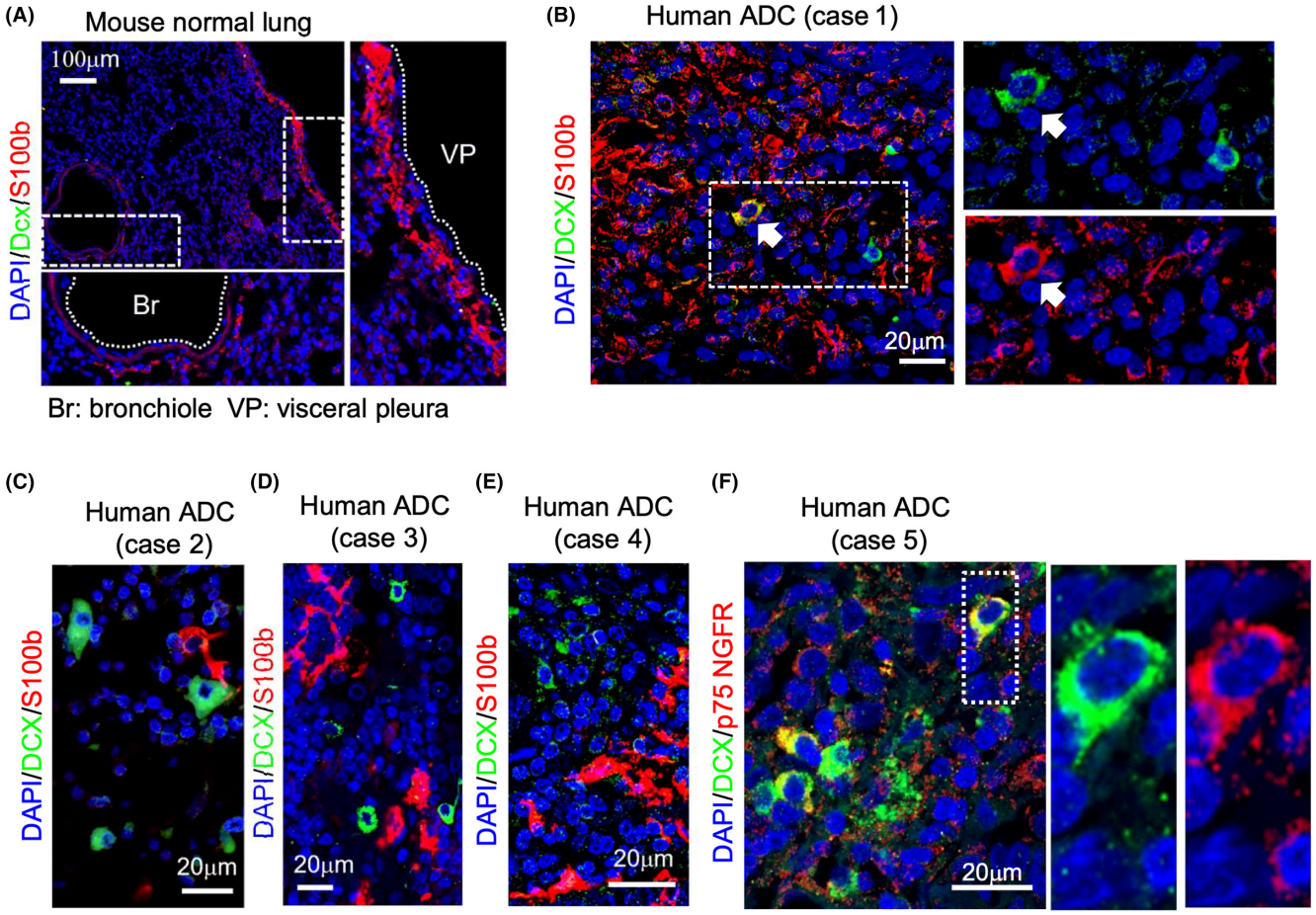

FIGURE 2 DCX-positive cells in lung cancer tissue express Schwann cell markers. (A) Representative image of immunofluorescent analyses using anti-DCX and anti-S100β antibodies on mouse normal lung tissue. Br, bronchiole; VP, visceral pleura. Scale bar: 100 μm. $n = 2$. (B–E) Representative images of immunofluorescent analyses using antibodies against DCX and S100β in human lung adenocarcinoma cancer tissues. Scale bars: 20 μm. (F) Immunofluorescence analysis using antibodies against DCX and another Schwann cell marker p75NGFR. Scale bar: 20 μm.

tdTomato-positive cells in a mouse model of lung cancer (Figure 4B). To examine whether the forced expression of YAP can dedifferentiate Schwann cells, we exogenously overexpressed YAP in mouse strain IMS-32 Schwann cells to generate yNSCs. IMS-32 cells were infected with lentiviruses expressing rtTA/tetON-GFP or rtTA/tetON-YAP and cultured in a Schwann cell maintenance medium with or without doxycycline for 2 weeks. Sphere formation was observed only in IMS-32 cells infected with rtTA/tetON-YAP and cultured in a medium containing doxycycline (Figure 4C). According to a previous report, Schwann cells acquire sphere-forming ability when cultured in serum-free medium containing epidermal growth factor (EGF) and fibroblast growth factor-2 (bFGF).[31] When IMS-32 cells were cultured in the same manner, they acquired a sphere-forming ability (Figure 4D; induced neurosphere-forming cells (iNSC)). Importantly, the loss of YAP/TAZ resulted in a deficit in the acquisition (Figure S2). Western blotting of cell extracts before and after acquiring sphere-forming ability revealed that Dcx expression was upregulated in samples after acquiring sphere-forming ability (Figure 4E). Furthermore, the expression levels of Axl and Cyr61 increased in the samples after acquiring sphere-forming ability (Figure 4E). Immunofluorescence analysis revealed that Yap activation and Dcx expression acquisition occurred after the dedifferentiation of IMS-32 cells (Figure 4F). These data indicated that Schwann cells acquired the new traits via YAP/TAZ activation in lung cancer tissues.

3.5 | DCX-positive cells in lung cancer tissue acquire sympathetic neuron-like properties

We thereafter examined the role of the new traits of Schwann cell populations, including DCX-positive cells, in lung cancer tissues. DCX-positive cells represent an early stage of differentiation within the nervous system.[35] These cells can differentiate into various lineages in the normal nervous system. Previous reports have shown that DCX-positive cells in prostate cancer tend to differentiate into sympathetic lineages, as demonstrated by immunofluorescence analysis.[27] Moreover, Schwann cell precursors were identified as the origin of adrenergic adrenal medullary chromaffin cells.[36] Accordingly, we hypothesized that DCX-positive Schwann cells in lung cancer tissues expressed catecholamine synthase.

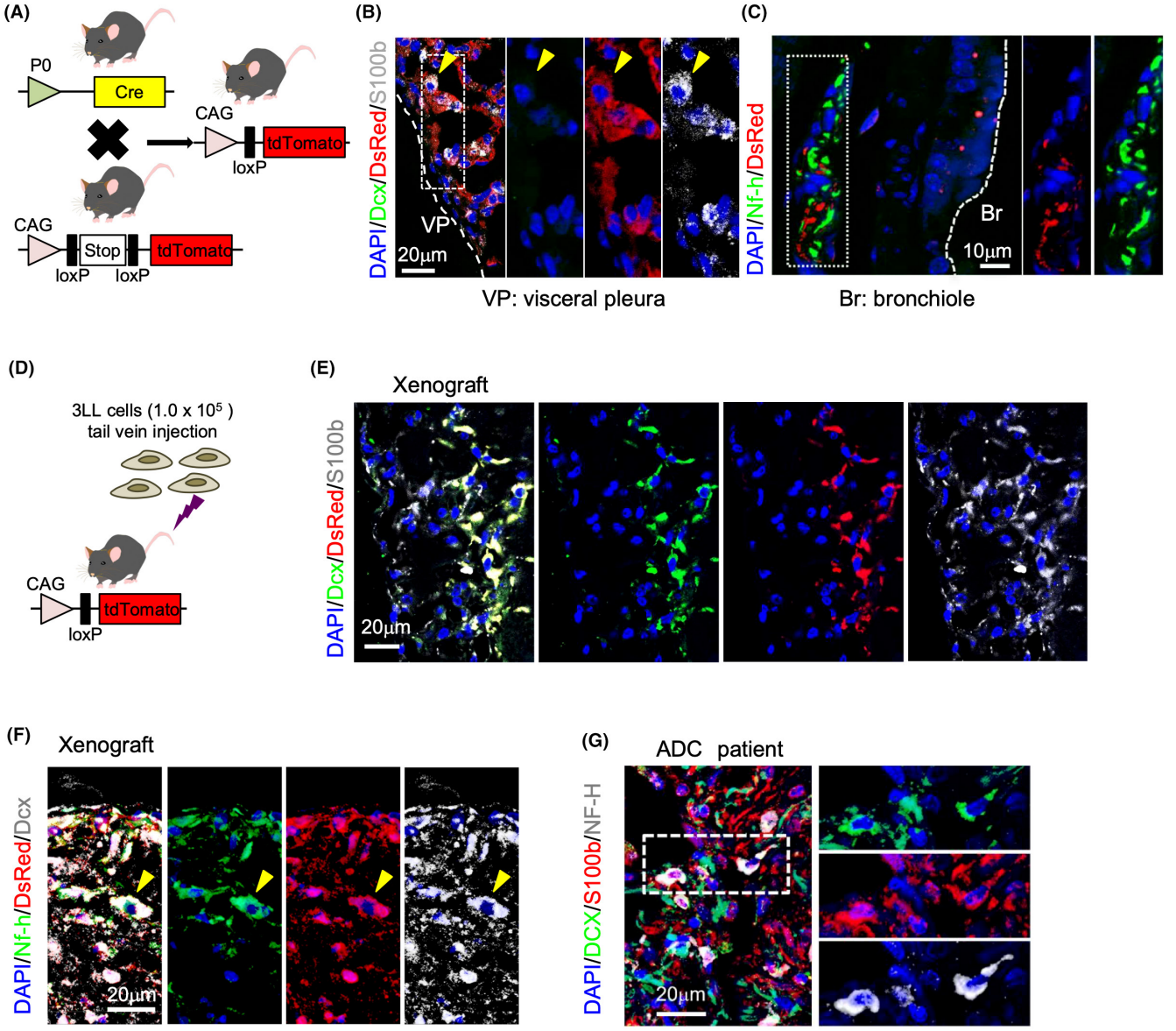

FIGURE 3 Lineage-tracing experiments reveal that Schwann cells express DCX in lung cancer tissue. (A) Cartoon describing the genetic background of the transgenic mouse used in a lineage-tracing experiment. (B) Representative image of immunofluorescence analysis of the normal lung from *P0-cre/loxP-stop-loxP-tdTomato* mouse using anti-DCX, anti-S100β, and anti-DsRed antibodies. Scale bar: 20 μm. $n = 2$. (C) Representative image of immunofluorescence analysis of normal lung from *P0-cre/loxP-stop-loxP-tdTomato* mice using antibodies against NF-H and DsRed. Scale bar: 10 μm. $n = 2$. (D) Cartoon describing the establishment of a lung cancer model using a 3LL cell line and a *P0-cre/loxP-stop-loxP-tdTomato* mouse line. (E) Representative image of immunofluorescence analysis of the lung cancer model mouse using a *P0-cre/loxP-stop-loxP-tdTomato* mouse line and antibodies against DCX, S100β, and DsRed. Scale bar: 20 μm. $n = 3$. (F) Representative image of an immunofluorescence analysis of the lung cancer model mouse using a *P0-cre/loxP-stop-loxP-tdTomato* mouse line and antibodies against NF-H, DCX, and DsRed. Scale bar: 20 μm. $n = 3$. (G) Representative image of immunofluorescence analysis using anti-DCX, S100β, and NF-H antibodies on human lung adenocarcinoma specimen. Scale bar: 20 μm.

The catecholamine synthesis pathway is shown in Figure 5A. Immunofluorescence analyses using antibodies against these synthases in human lung cancer tissue revealed that some DCX-positive cells expressed TH, DDC, DbH, and PNMT (Figure 5B–E). Furthermore, immunofluorescence analyses using antibodies against noradrenaline and adrenaline confirmed that noradrenaline and adrenaline signals were observed in DCX-positive cells expressing catecholamine synthase (Figure 5C,E). Moreover, in a lineage-tracing experiment using *P0-cre/loxP-stop-loxP-tdTomato* mice, we confirmed that some tdTomato-positive cells express a group of catecholamine synthases (Figure 5F–I), noradrenaline, and adrenaline (Figure 5J,K). Importantly, neither the expression of the catecholamine synthase family nor any signal of catecholamines was detected in Schwann cells in normal lung tissue

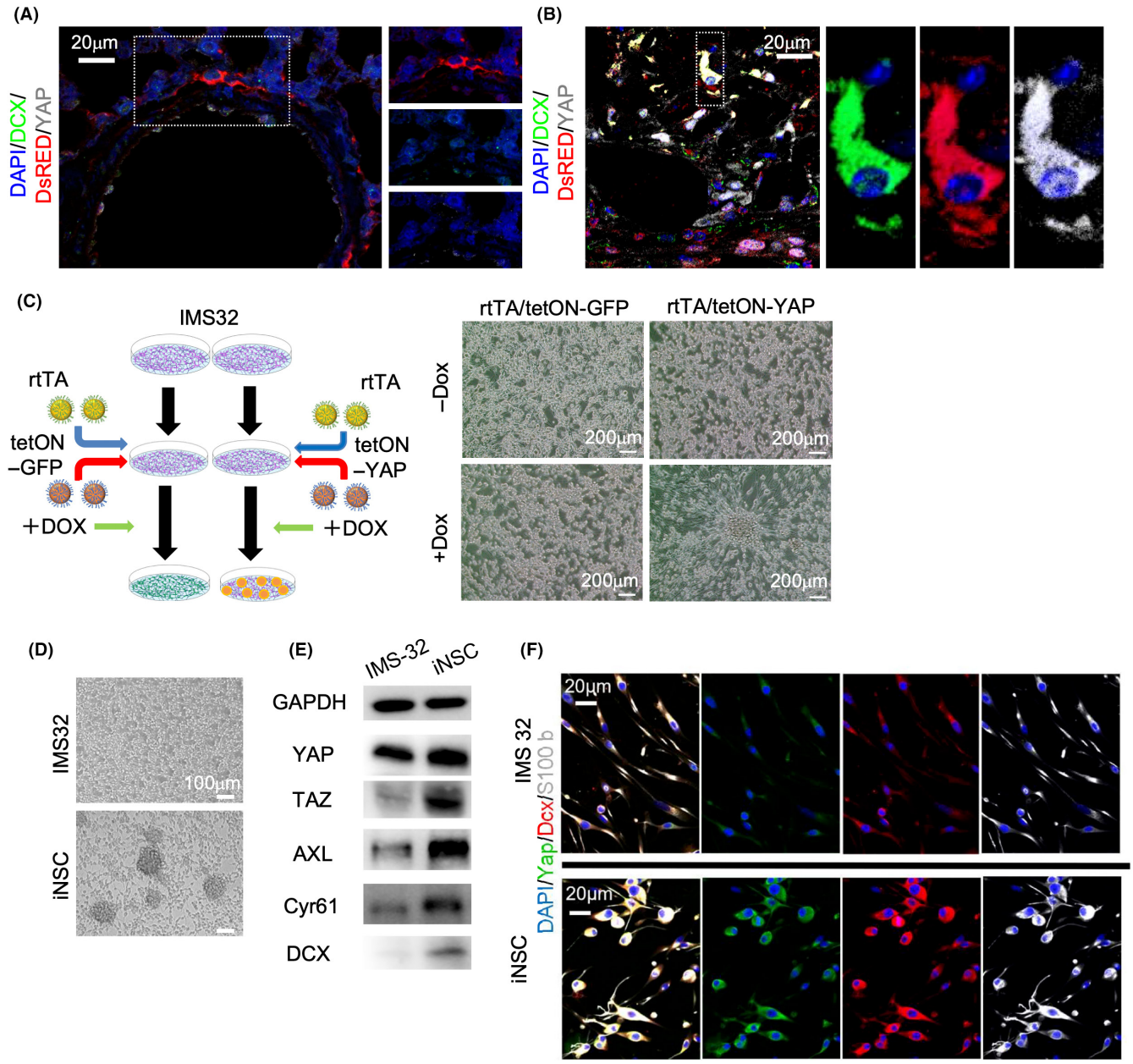

FIGURE 4 Schwann cells acquire DCX positivity by activation of YAP/TAZ signaling. (A) Representative image of an immunofluorescence analysis of the lung from *P0-cre/loxP-stop-loxP-tdTomato* mouse using antibodies against DCX, YAP, and DsRed. Scale bar: 20 μm. $n=2$. (B) Representative image of the immunofluorescence analysis of a lung cancer mouse model using a *P0-cre/loxP-stop-loxP-tdTomato* mouse line and antibodies against DCX, YAP, and DsRed. Scale bar: 20 μm. $n=3$. (C) Cartoon describing the procedure for the induction of yNSC from IMS-32 cells (*left*) and representative images of IMS-32 infected with lentiviruses expressing rtTA/tetON-GFP or rtTA/tetON-YAP and cultured in a medium containing doxycycline for 2 weeks (*right*). Scale bars: 200 μm. $n=4$. (D) Representative images of IMS-32 cultured in Schwann cell medium (*upper panel*) and IMS-32 dedifferentiated in neurobasal medium supplemented with B-27, N-2, EGF, bFGF, and heparin (*lower panel*: iNSC = induced neurosphere-forming cells). Scale bars: 100 μm. $n=4$. (E) Western blotting images of Dcx, Yap, Taz, Axl, Cyr61, and Gapdh in IMS-32 and dedifferentiated IMS-32 cell (iNSC) lysates. Full scans of the western blots are shown in Figure S5. (F) Representative image of immunofluorescence analysis of IMS-32 maintained in Schwann cell medium (*upper panels*) and IMS-32 dedifferentiated in neurobasal medium (*lower panels*: iNSC) using antibodies against Yap, Dcx, and S100β. Scale bars: 20 μm. $n=2$.

(Figure S3). Finally, in vitro validation using IMS-32 showed that adrenaline synthesis was not observed before the induction of activation, whereas adrenaline synthesis was observed in cells after activation (Figure 5L). These data suggest that Schwann cells acquire sympathetic neuron-like properties and synthesize catecholamines in lung cancer tissue.

3.6 | Cancer-associated Schwann cells exacerbate lung cancer cells by adrenaline in a YAP/TAZ-dependent manner

Thus far, we have shown that Schwann cells can acquire DCX positivity and catecholamine-synthesizing capacity in lung cancer

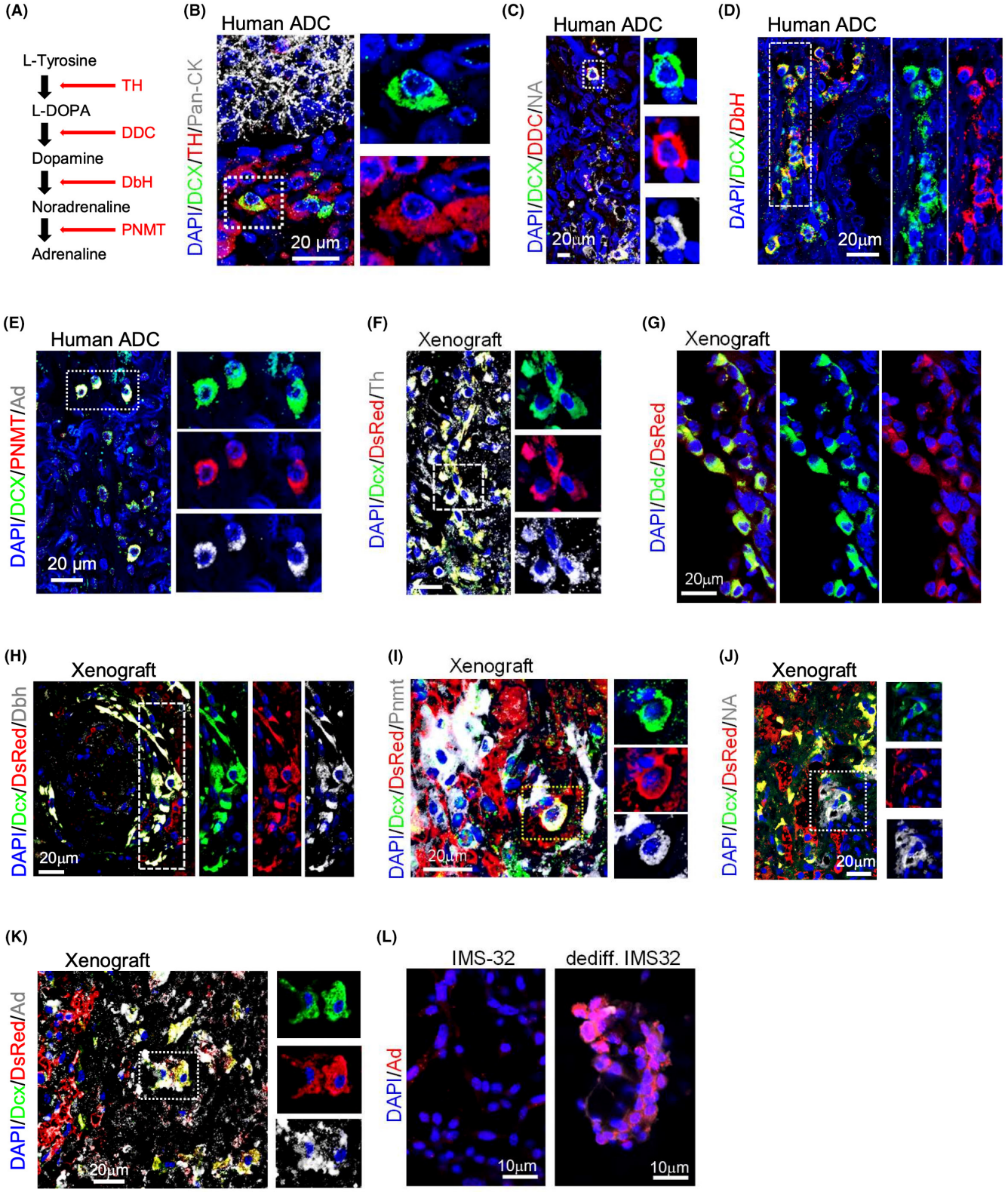

tissue. Hereafter, we define these cells as CAS, which are activated Schwann cells in cancer tissues. We investigated whether CAS, which has acquired the ability to produce catecholamines, influence the behavior of lung cancer cells. In recent years, catecholamines, components of the cancer microenvironment, have become increasingly important in cancer biology. For example, a stress-induced elevation of blood adrenaline reportedly promotes cancer progression in breast cancer.[20] Previously, we demonstrated that the adrenaline treatment of MPNST cells enhanced cancer stemness via YAP/TAZ.[23] Noradrenaline treatment reportedly enhances drug resistance.[21] As shown in Figure 5, CAS synthesizes noradrenaline and adrenaline. To test whether the

FIGURE 5 Schwann cells acquire sympathetic neuron-like properties in lung cancer tissues. (A) Cartoon describing the molecular pathway of catecholamine synthesis. (B–E) Representative images of immunofluorescent analyses on human lung adenocarcinoma specimens using antibodies against DCX, tyrosine hydroxylase (TH), and pan-cytokeratin (B), antibodies against DCX, DOPA decarboxylase (DDC), and noradrenaline (C), antibodies against DCX and dopamine beta-hydroxylase (DbH) (D), and antibodies against DCX, phenylethanolamine *N*-methyltransferase (PNMT), and adrenaline (E). Scale bars: 20 μm. $n = 3$, each. (F–I) Representative image of immunofluorescence analysis of the 3LL lung cancer mouse model using a *P0-cre/loxP-stop-loxP-tdTomato* mouse line and antibodies against Dcx, DsRed, and Th (F), antibodies against Ddc and DsRed (G), antibodies against Dcx, DsRed, and DbH (H), and antibodies against Dcx, DsRed, and Pnmt (I). Scale bars: 20 μm. $n = 2$, each. (J, K) Representative image of the immunofluorescence analysis of the 3LL lung cancer mouse model using a *P0-cre/loxP-stop-loxP-tdTomato* mouse line and antibodies against Dcx, DsRed, and noradrenaline (J), and antibodies against Dcx, DsRed, and adrenaline (K). Scale bars: 20 μm. $n = 2$, each. (L) Representative image of the immunofluorescence analysis of IMS-32 and dedifferentiated IMS-32 using antibodies against adrenaline. Scale bars: 10 μm. $n = 2$.

catecholamines synthesized by CAS could affect the surrounding lung cancer cells and promote lung cancer progression, we first tested the self-renewal ability of lung cancer cells using a medium containing L-tyrosine, L-DOPA, dopamine, noradrenaline, and adrenaline (10 nM each). We performed a sphere formation assay using HCC827, HCC4006, H520, and HARA-B4 cells in the abovementioned medium. Of these cells, adrenaline significantly enhanced the self-renewal capacity of all lung cancer cell lines (Figure 6A). Furthermore, adrenaline treatment markedly increased the drug resistance capacity of HCC827 and HCC4006 cells to gefitinib, a selective tyrosine kinase inhibitor against the EGF receptor (Figure 6B). Interestingly, adrenaline treatment did not affect the drug resistance capacity of these cells to cisplatin, one of the key cytotoxic drugs in lung cancer treatment, suggesting that the effect of adrenaline on the drug resistance capacity is specific for gefitinib (Figure S4). We previously reported that the adrenaline treatment of MPNST cells enhanced YAP/TAZ activity.[23] As YAP/TAZ is widely recognized as a factor that defines cancer stemness and drug resistance in various cancer types, including lung cancer, breast cancer, and malignant brain tumors,[37–39] we tested whether YAP/TAZ was enhanced by adrenaline treatment in lung cancer cells. We confirmed that adrenaline treatment increased YAP protein levels in HCC4006 cells (Figure 6C, full scans of the western blots are shown in Figure S5). In human lung cancer specimens, an immunofluorescence analysis using anti-YAP and anti-S100β antibodies revealed that the nuclear localization of YAP, which indicates the activated state of YAP, was observed in pan-cytokeratin-positive lung cancer cells proximal to CAS (Figure 6D, arrowheads), whereas YAP nuclear localization was not observed in lung cancer cells that were not proximal to CAS (Figure 6D). These data suggest that adrenaline derived from CAS may promote YAP activity in lung cancer cells, thereby enhancing their stemness and drug resistance potential.

Finally, we investigated whether CAS affected patient prognosis. The immunofluorescence analyses of 33 lung cancer patients who underwent surgery followed by chemotherapy at Okayama University Hospital showed that the area ratio of Schwann cells stained with S100β was significantly higher in patients with recurrent disease than in those without recurrent disease (Figure 6E,F). The 5-year recurrence-free rates of these patients are shown in Figure 6G. We did not find any significant correlation between the clinicopathological characteristics of these patients and the abundance of S100β-positive Schwann cells in the cohort. These data suggest that CAS is involved in the recurrence of lung cancer, probably due to enhanced chemoresistance (Figure 7).

4 | DISCUSSION

This study found that Schwann cells in lung cancer tissue showed DCX positivity and acquired sympathetic neuron-like properties, as shown by the expression of catecholamine synthases. These Schwann cells synthesized noradrenaline and adrenaline and activated YAP in neighboring cancer cells. Validation using lung cancer cell lines showed that only adrenaline, among the components of the catecholamine-synthesizing pathway, enhanced the self-renewal capacity and that adrenaline treatment markedly enhanced the chemoresistant potential of lung cancer cells. During the acquisition of new traits in Schwann cells, the activation of YAP/TAZ, a Hippo pathway transducer, was observed. Similar to a previous study describing that the transient overexpression of YAP/TAZ in neurons led to the dedifferentiation into yNSCs, we succeeded in inducing yNSCs from Schwann cells. The molecular mechanism of the de novo dedifferentiation of Schwann cells in lung cancer tissues is considered to be influenced by the cytokines secreted by cancer cells. For example, nerve growth factor (NGF), a cancer-secreted growth factor and ligand for NGFR, which is a surface marker of Schwann cells, has been reported to activate YAP,[40] suggesting that NGF derived from cancer cells activates YAP/TAZ via NGFR on the Schwann cell surface to induce dedifferentiation. As fibroblasts are transformed by cancer cells into cancer-associated fibroblasts, and their newly acquired traits promote cancer, we named Schwann cells transformed by cancer cells as CAS. Further studies on the detailed molecular mechanisms by which cancer cells induce CAS and the effects of CAS on cancer cells, beyond those described in this study, are warranted.

In Figure 2, we observed that, in normal lung tissue, Schwann cells are abundant in the peribronchial area and underneath the visceral pleura. These areas are rich in nerve fibers, including sensory and autonomic nerves. Depending on the subtypes of lung cancer, for example, adenocarcinoma tends to occur in the peripheral region of the lung, which may be partly affected by Schwann cells underneath the visceral pleura. Squamous-cell carcinoma tends to occur in the central region of the lung and may be affected by peribronchial

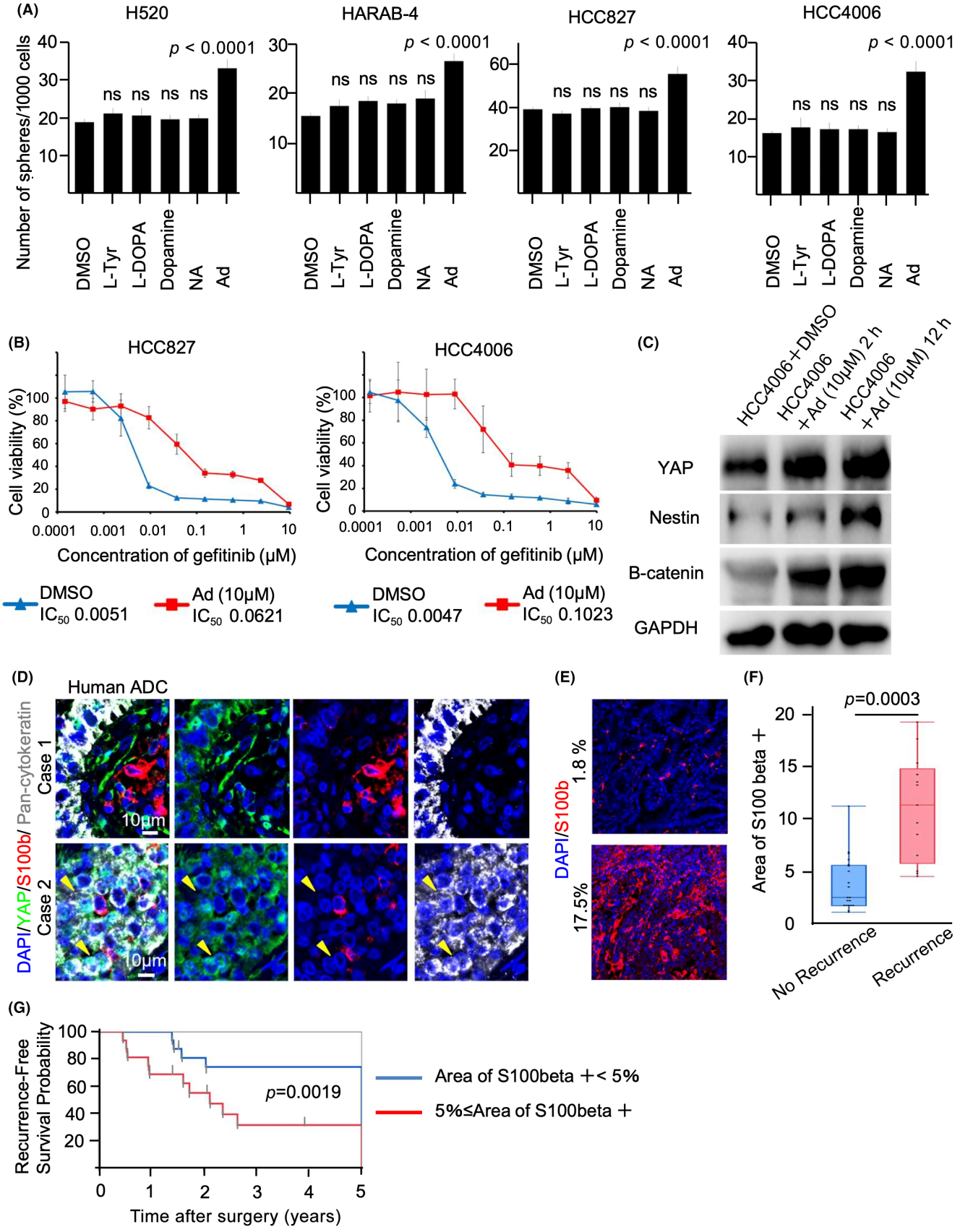

Schwann cells. The role of the sympathetic neuron-like characteristics of CAS in different histopathological subtypes of lung cancer requires further analysis.

Schwann cells are activated during nerve injury and acquire plasticity.[41,42] There is an increasing amount of evidence that several factors from cancer cells activate Schwann cells and that the newly

FIGURE 6 Cancer-associated Schwann cells exacerbate lung cancer cells by adrenaline in a YAP/TAZ-dependent manner and affect the prognosis of patients with lung cancer. (A) Quantification of self-renewal capacity of lung cancer cell lines treated with catecholamines. The dose of each chemical concentration is 10 nM ($n=4$, error bars indicate mean ± standard deviation (SD)). (B) Representative graphs of cell viability in the presence of serially diluted gefitinib (concentration range: 0, 0.00015, 0.00061, 0.00244, 0.00977, 0.03906, 0.15625, 0.625, 2.5, and 10 μM) with or without adrenaline (10 μM) ($n=8$, error bars indicate mean ± SD). An IC_{50} of HCC827 treated with dimethyl sulfoxide (DMSO) and adrenaline yields a value of 0.0051 μM and 0.0621 μM, respectively. An IC_{50} of HCC4006 treated with DMSO and adrenaline yields a value of 0.0047 μM and 0.1023 μM, respectively. (C) Western blotting images of YAP, NESTIN, β-CATENIN, and GAPDH in HCC4006 treated with adrenaline for 0, 2, or 12 h. Full scans of the western blots are shown in Figure S5. (D) Representative images of immunofluorescent analyses on human lung adenocarcinoma specimens using antibodies against YAP, pan-cytokeratin, and S100β. Scale bars: 10 μm. (E) Representative images of immunofluorescent analyses on human lung adenocarcinoma specimens using antibodies against S100β. The numbers indicate the percentage of the S100β-stained area. Scale bars: 20 μm. (F) Boxplot graph describing that the area of Schwann cells stained with S100β in the specimens of patients with recurrent lung cancer is significantly broader than that of patients without recurrence ($p=0.0003$). (G) Kaplan–Meier curves showing the 5-year recurrence-free survival of lung cancer patients stratified according to the area of Schwann cells stained with S100β ($p=0.0019$).

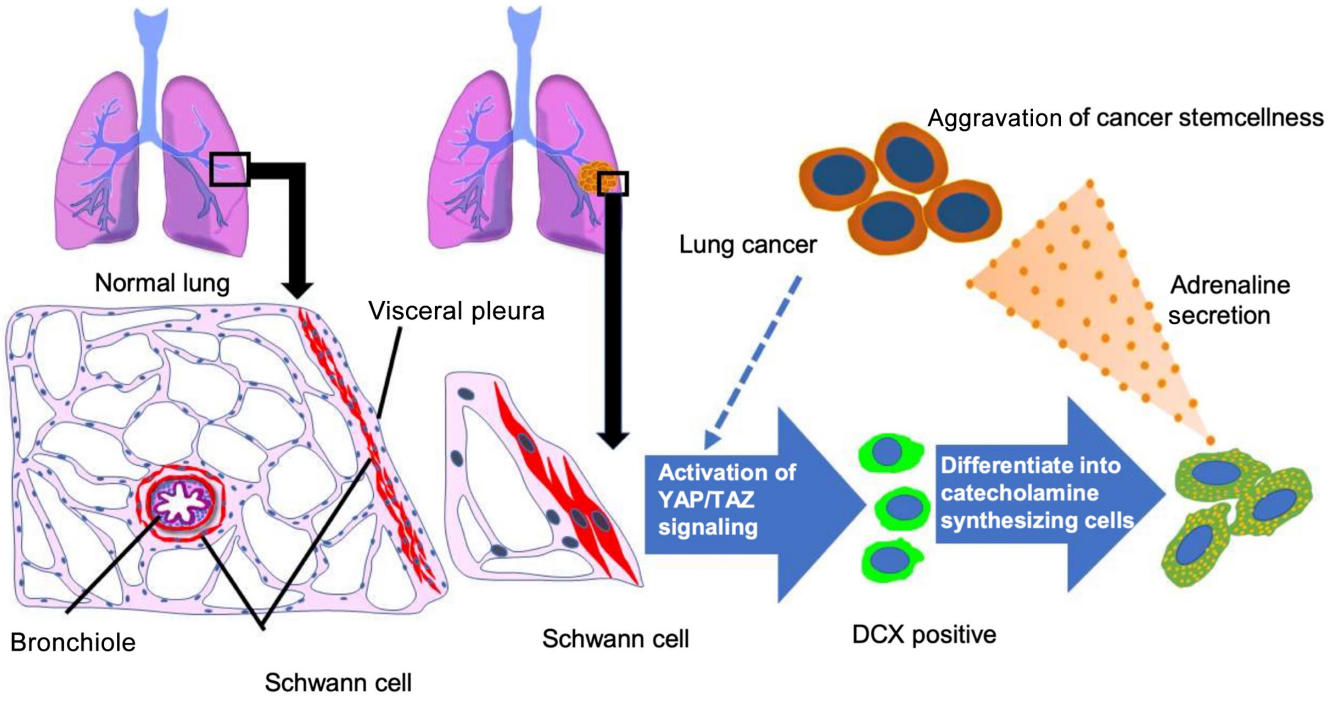

FIGURE 7 Summary of the results of this study. Schwann cells exist in the peri-bronchiole and visceral pleura in the normal lung. Upon stimulation from cancer cells, Schwann cells acquire DCX positivity and sympathetic neuron-like properties via the activation of YAP/TAZ signaling. Cancer-associated Schwann cells (CAS) express catecholamine-synthesizing enzymes and synthesize adrenaline, which may promote the cancer stemness of lung cancer cells close to CAS.

acquired traits of Schwann cells can affect the cancer cell characteristics. For example, Schwann cells reportedly promote cancer dispersion and invasion in pancreatic cancer.[43] In melanoma, melanoma cells convert Schwann cells from a static state to a repair-like state and make them support tumor growth.[44] In this study, we revealed that Schwann cells could be activated to DCX-positive cells and acquire catecholamine-synthesizing capacity in lung cancer tissues. Our data reveal that cancer cells can transform Schwann cells into CAS, which promotes chemoresistance of cancer cells. Such a reciprocal regulation of the adrenergic microenvironment sustained by CAS may be a candidate for cancer therapy. In particular, targeting YAP/TAZ can be a promising method to eliminate the CAS-dependent adrenergic microenvironment because YAP/TAZ plays a pivotal role both in CAS induction and in the cancer cell acquisition of chemoresistance.

AUTHOR CONTRIBUTIONS

Yusuke Otani: Data curation; formal analysis; funding acquisition; investigation; validation; visualization. **Haruyoshi Katayama:** Data curation; formal analysis; investigation; methodology; visualization; writing – review and editing. **Yidan Zhu:** Data curation; formal analysis; investigation; visualization. **Rongsheng Huang:** Formal analysis; investigation; methodology; writing – review and editing. **Takafumi Shigehira:** Formal analysis; investigation. **Kazuhiko Shien:** Writing – review and editing. **Ken Suzawa:** Methodology; resources; writing – review and editing. **Hiromasa Yamamoto:** Writing

– review and editing. **Tadahiko Shien:** Writing – review and editing. **Shinichi Toyooka:** Funding acquisition; project administration; writing – review and editing. **Atsushi Fujimura:** Conceptualization; data curation; formal analysis; funding acquisition; investigation; methodology; project administration; resources; supervision; validation; writing – original draft; writing – review and editing.

ACKNOWLEDGMENTS

We thank S. Piccolo for sharing the plasmids. We are grateful to the Central Research Laboratory, Okayama University Medical School for their support with confocal microscopy. We thank all members of our laboratory for their valuable comments. We also thank Editage for English language processing and editing.

FUNDING INFORMATION

This work was supported by a Grant-in-Aid for Scientific Research from the Ministry of Education, Culture, Sports, Sciences, and Technology of Japan (grant numbers: JP22K09004 to Y.O., JP23K06676 to A.F., and JP22H03162 to S.To.), the Japan Agency for Medical Research and Development (grant numbers: JP19cm0106143 and JP22cm0106179 to A.F.), and the Naito Foundation (A.F.).

CONFLICT OF INTEREST STATEMENT

All authors declare that they have no competing interests.

ETHICS STATEMENT

Approval of the research protocol by an Institutional Reviewer Board: Human lung cancer specimens, relevant information, and anonymized medical data were obtained from the Okayama University Hospital following approval by the ethical committee of the hospital (approval number: 1603–066). Specimens of human adult normal lung tissue were purchased from Cosmo Bio (catalog number: T2234152).

Informed Consent: Informed consent was obtained through the website of the Okayama University Hospital (http://ninai.med.okayama-u.ac.jp/wp-content/uploads/2022/05/3533e8e3991811553df0d81b4b96caaa.pdf) with an opt-out option.

Registry and the Registration No. of the study/trial: N/A.

Animal Studies: Animal experiments were performed with permission from and in accordance with all guidelines put forth by the committees of the Okayama University (approval number: OKU-2021726 for animal usage and 20,028 for recombinant DNA experiments on transgenic mice).

ORCID

Kazuhiko Shien https://orcid.org/0000-0002-4959-4220
Hiromasa Yamamoto https://orcid.org/0000-0002-5330-5460
Tadahiko Shien https://orcid.org/0000-0003-3202-5512
Shinichi Toyooka https://orcid.org/0000-0002-7588-6745
Atsushi Fujimura https://orcid.org/0000-0002-8638-5460

REFERENCES

1. Johnson M, Garassino MC, Mok T, Mitsudomi T. Treatment strategies and outcomes for patients with EGFR-mutant non-small cell lung cancer resistant to EGFR tyrosine kinase inhibitors: focus on novel therapies. *Lung Cancer*. 2022;170:41-51. doi:10.1016/j.lungcan.2022.05.011
2. Gelatti ACZ, Drilon A, Santini FC. Optimizing the sequencing of tyrosine kinase inhibitors (TKIs) in epidermal growth factor receptor (EGFR) mutation-positive non-small cell lung cancer (NSCLC). *Lung Cancer*. 2019;137:113-122. doi:10.1016/j.lungcan.2019.09.017
3. Gao J, Li HR, Jin C, Jiang JH, Ding JY. Strategies to overcome acquired resistance to EGFR TKI in the treatment of non-small cell lung cancer. *Clin Transl Oncol*. 2019;21(10):1287-1301. doi:10.1007/s12094-019-02075-1
4. Sperduto PW, Yang TJ, Beal K, et al. Estimating survival in patients with lung cancer and brain metastases: An update of the graded prognostic assessment for lung cancer using molecular markers (lung-molGPA). *JAMA Oncol*. 2017;3(6):827-831. doi:10.1001/jamaoncol.2016.3834
5. Zheng Y, Wang L, Yin L, et al. Lung cancer stem cell markers as therapeutic targets: An update on signaling pathways and therapies. *Front Oncol*. 2022;12:873994. doi:10.3389/fonc.2022.873994
6. Li L, Li JC, Yang H, et al. Expansion of cancer stem cell pool initiates lung cancer recurrence before angiogenesis. *Proc Natl Acad Sci USA*. 2018;115(38):E8948-E8957. doi:10.1073/pnas.1806219115
7. Césaire M, Montanari J, Curcio H, et al. Radioresistance of non-small cell lung cancers and therapeutic perspectives. *Cancers (Basel)*. 2022;14(12):2829. doi:10.3390/cancers14122829
8. Sutherland KD, Ireland AS, Oliver TG. Killing SCLC: insights into how to target a shapeshifting tumor. *Genes Dev*. 2022;36(5–6):241-258. doi:10.1101/gad.349359.122
9. Yoshida GJ, Saya H. Molecular pathology underlying the robustness of cancer stem cells. *Regen Ther*. 2021;17:38-50. doi:10.1016/j.reth.2021.02.002
10. Wang J, Ma Y, Long Y, Chen Y. Extracellular vesicle derived from mesenchymal stem cells have bidirectional effects on the development of lung cancer. *Front Oncol*. 2022;12:914832. doi:10.3389/fonc.2022.914832
11. Nayak A, Warrier NM, Kumar P. Cancer stem cells and the tumor microenvironment: targeting the critical crosstalk through Nanocarrier systems. *Stem Cell Rev Rep*. 2022;18:2209-2233. doi:10.1007/s12015-022-10426-9
12. Qiao L, Chen Y, Liang N, et al. Targeting epithelial-to-mesenchymal transition in Radioresistance: Crosslinked mechanisms and strategies. *Front Oncol*. 2022;12:775238. doi:10.3389/fonc.2022.775238
13. Mudra SE, Sadhukhan P, Ugurlu MT, Alam S, Hoque MO. Therapeutic targeting of cancer stem cells in lung, head and neck, and bladder cancers. *Cancers (Basel)*. 2021;13(20):5098. doi:10.3390/cancers13205098
14. Lee PJ, Ho CC, Ho H, et al. Tumor microenvironment-based screening repurposes drugs targeting cancer stem cells and cancer-associated fibroblasts. *Theranostics*. 2021;11(19):9667-9686. doi:10.7150/thno.62676
15. Borriello L, Coste A, Traub B, et al. Primary tumor associated macrophages activate programs of invasion and dormancy in disseminating tumor cells. *Nat Commun*. 2022;13(1):626. doi:10.1038/s41467-022-28076-3
16. Sun H, Li Q, Song Z, Li C. Hypoxia induction of SH2D3A triggers malignant progression of lung cancer. *Stem Cell Res*. 2022;58:102630. doi:10.1016/j.scr.2021.102630
17. Parker TM, Gupta K, Palma AM, et al. Cell competition in intratumoral and tumor microenvironment interactions. *EMBO J*. 2021;40(17):e107271. doi:10.15252/embj.2020107271
18. Moosavi F, Giovannetti E, Peters GJ, Firuzi O. Combination of HGF/MET-targeting agents and other therapeutic strategies in cancer. *Crit Rev Oncol Hematol*. 2021;160:103234. doi:10.1016/j.critrevonc.2021.103234
19. Yamamoto T, Fujimura A, Wei FY, et al. 2-Methylthio conversion of N6-Isopentenyladenosine in mitochondrial tRNAs by CDK5RAP1

promotes the maintenance of glioma-initiating cells. *iScience*. 2019;21:42-56. doi:10.1016/j.isci.2019.10.012
20. Cui B, Luo Y, Tian P, et al. Stress-induced epinephrine enhances lactate dehydrogenase a and promotes breast cancer stem-like cells. *J Clin Invest*. 2019;129(3):1030-1046. doi:10.1172/JCI121685
21. Nilsson MB, Sun H, Diao L, et al. Stress hormones promote EGFR inhibitor resistance in NSCLC: implications for combinations with β-blockers. *Sci Transl Med*. 2017;9(415):eaao4307. doi:10.1126/scitranslmed.aao4307. Erratum in: Sci Transl Med 2019 May 22;11(493): PMID: 29118262.
22. Silva D, Quintas C, Gonçalves J, Fresco P. Contribution of adrenergic mechanisms for the stress-induced breast cancer carcinogenesis. *J Cell Physiol*. 2022;237(4):2107-2127. doi:10.1002/jcp.30707
23. Huang R, Fujimura A, Nakata E, et al. Adrenergic signaling promotes the expansion of cancer stem-like cells of malignant peripheral nerve sheath tumors. *Biochem Biophys Res Commun*. 2021;557:199-205. doi:10.1016/j.bbrc.2021.03.172
24. Zanconato F, Cordenonsi M, Piccolo S. YAP and TAZ: a signalling hub of the tumour microenvironment. *Nat Rev Cancer*. 2019;19(8):454-464. doi:10.1038/s41568-019-0168-y
25. Cordenonsi M, Zanconato F, Azzolin L, et al. The hippo transducer TAZ confers cancer stem cell-related traits on breast cancer cells. *Cell*. 2011;147(4):759-772. doi:10.1016/j.cell.2011.09.048
26. Castellan M, Guarnieri A, Fujimura A, et al. Single-cell analyses reveal YAP/TAZ as regulators of stemness and cell plasticity in glioblastoma. *Nat Cancer*. 2021;2(2):174-188. doi:10.1038/s43018-020-00150-z
27. Mauffrey P, Tchitchek N, Barroca V, et al. Progenitors from the central nervous system drive neurogenesis in cancer. *Nature*. 2019;569(7758):672-678. doi:10.1038/s41586-019-1219-y
28. Audrit KJ, Delventhal L, Aydin Ö, Nassenstein C. The nervous system of airways and its remodeling in inflammatory lung diseases. *Cell Tissue Res*. 2017;367(3):571-590. doi:10.1007/s00441-016-2559-7
29. Bolívar S, Navarro X, Udina E. Schwann cell role in selectivity of nerve regeneration. *Cells*. 2020;9(9):2131. doi:10.3390/cells9092131
30. Gordon T. Peripheral nerve regeneration and muscle Reinnervation. *Int J Mol Sci*. 2020;21(22):8652. doi:10.3390/ijms21228652
31. Stierli S, Imperatore V, Lloyd AC. Schwann cell plasticity-roles in tissue homeostasis, regeneration, and disease. *Glia*. 2019;67(11):2203-2215. doi:10.1002/glia.23643
32. Boerboom A, Dion V, Chariot A, Franzen R. Molecular mechanisms involved in Schwann cell plasticity. *Front Mol Neurosci*. 2017;10:38. doi:10.3389/fnmol.2017.00038
33. Suarez-Mier GB, Buckwalter MS. Glial fibrillary acidic protein-expressing glia in the mouse lung. *ASN Neuro*. 2015;7(5):1759091415601636. doi:10.1177/1759091415601636
34. Panciera T, Azzolin L, Fujimura A, et al. Induction of expandable tissue-specific stem/progenitor cells through transient expression of YAP/TAZ. *Cell Stem Cell*. 2016;19(6):725-737. doi:10.1016/j.stem.2016.08.009
35. Klein B, Mrowetz H, Kreutzer C, et al. DCX$^+$ neuronal progenitors contribute to new oligodendrocytes during remyelination in the hippocampus. *Sci Rep*. 2020;10(1):20095. doi:10.1038/s41598-020-77115-w
36. Furlan A, Dyachuk V, Kastriti ME, et al. Multipotent peripheral glial cells generate neuroendocrine cells of the adrenal medulla. *Science*. 2017;357(6346):eaal3753. doi:10.1126/science.aal3753
37. Horie M, Saito A, Ohshima M, Suzuki HI, Nagase T. YAP and TAZ modulate cell phenotype in a subset of small cell lung cancer. *Cancer Sci*. 2016;107(12):1755-1766. doi:10.1111/cas.13078
38. Kim YJ, Jang SK, Hong SE, et al. Knockdown of YAP/TAZ sensitizes tamoxifen-resistant MCF7 breast cancer cells. *Biochem Biophys Res Commun*. 2022;601:73-78. doi:10.1016/j.bbrc.2022.02.083
39. Casati G, Giunti L, Iorio AL, Marturano A, Galli L, Sardi I. Hippo pathway in regulating drug resistance of glioblastoma. *Int J Mol Sci*. 2021;22(24):13431. doi:10.3390/ijms222413431
40. Wang L, Li J, Wang R, et al. NGF signaling interacts with the hippo/YAP pathway to regulate cervical cancer progression. *Front Oncol*. 2021;11:688794. doi:10.3389/fonc.2021.688794
41. Takagi T, Ishii K, Shibata S, et al. Schwann-spheres derived from injured peripheral nerves in adult mice – their in vitro characterization and therapeutic potential. *PLoS One*. 2011;6(6):e21497. doi:10.1371/journal.pone.0021497
42. Wei Z, Shu S, Zhang M, et al. A subpopulation of Schwann cell-like cells with nerve regeneration signatures is identified through single-cell RNA sequencing. *Front Physiol*. 2021;12:637924. doi:10.3389/fphys.2021.637924
43. Deborde S, Gusain L, Powers A, et al. Reprogrammed Schwann cells organize into dynamic tracks that promote pancreatic cancer invasion. *Cancer Discov*. 2022;12(10):2454-2473. doi:10.1158/2159-8290.CD-21-1690
44. Kastriti ME, Faure L, Von Ahsen D, et al. Schwann cell precursors represent a neural crest-like state with biased multipotency. *EMBO J*. 2022;41(17):e108780. doi:10.15252/embj.2021108780

SUPPORTING INFORMATION

Additional supporting information can be found online in the Supporting Information section at the end of this article.

How to cite this article: Otani Y, Katayama H, Zhu Y, et al. Adrenergic microenvironment driven by cancer-associated Schwann cells contributes to chemoresistance in patients with lung cancer. *Cancer Sci*. 2024;00:1-13. doi:10.1111/cas.16164